12. Kolmogoroff, A. N., *Dokl. Akad. Nauk SSSR*, **66**, 825 (1949).
13. Sleicher, C. A., *A.I.Ch.E. J.*, **8**, 471 (1961).
14. Calderbank, P. H., *Trans. Inst. Chem. Engrs.*, **36**, 443 (1958).
15. Vermeulen, T., G. M. Williams, and G. E. Langlois, *Chem. Eng. Progr.*, **51**, 85F (1955).
16. Epstein, P. S., and M. S. Plesset, *J. Chem. Phys.*, **18**, 1505 (1950).
17. Hinze, J. O., "Turbulence," McGraw-Hill, New York (1959).
18. Bagnold, R. A., *Phil. Trans. Roy. Soc. (London)*, **249**, 235 (1956); *Proc. Roy. Soc.*, **A225**, 49 (1954).

Manuscript received November 2, 1964; revision received April 28, 1965; paper accepted April 30, 1965.

Effects of Mixing on Chain Reactions in Isothermal Photoreactors

FRANK B. HILL and RICHARD M. FELDER

Brookhaven National Laboratory, Upton, New York

An analytical study of the interaction of mixing, radiation attenuation, and chemical kinetics in isothermal photoreactors is presented. For a particular chain reaction mechanism in the presence of stationary state kinetics and low conversion, the conditions required for the existence of mixing effects are formally stated, and the direction of change of conversion and quantum yield resulting from the introduction of mixing is established. Calculated results are presented for monoenergetic, unidirectional sources. Factors considered include mode of chain termination, radiation attenuation law, photoreactor geometry, state of mixing, and reactor optical thickness. Chemical and mixing time scale considerations are discussed.

Much attention has been given in recent years to the effects of mixing on chemical reactor performance. Most of the work done has involved simple, single-step thermal reactions. Very little has been done on mixing as it affects the performance of photoreactors, especially in the presence of typical complex reactions of industrial interest.

Many sources exist that suggest that mixing may under certain circumstances be beneficial to photoreactor performance (*1* to *5*). While it is not always clear what the precise cause of improved performance is, the introduction of turbulence seems to be a factor in all cases, the turbulence arising from high flow rates, stirring or agitation, or the use of baffles. In the present paper an interaction of chemical kinetics, radiation attenuation, and mixing in isothermal systems is discussed, which may be related to the reported improvement in photoreactor performance. In the course of describing the interaction it is necessary to treat the absence of mixing as well as its presence. Interesting effects are found in both cases. The interaction may in principle be found both in photochemical reactors and in radiation chemical reactors. Both types of reactor will therefore be implied in the use of the term *photoreactor*.

Photochemists have been aware of the interaction for some time. It was evidently first described by Bhagwat and Dhar (*6*) in 1932. These authors showed that two conditions had to be satisfied in order for a mixing effect to exist: (1) the local reaction rate had to depend on a power of the locally absorbed radiation intensity other than unity, and (2) the absorbing reactant layer had to be optically thick. It was shown mathematically for a photoreaction whose rate depended on a power of the absorbed intensity less than one that stirring increased the observed rate of the reaction. The greater the optical density of the reaction mixture, the greater the increase in rate.*

To the two conditions set forth by Bhagwat and Dhar a third must be added, which arises from consideration of reaction mechanism and relative time scales of chemical kinetics and mixing processes, as will be seen below.

Information on reaction mechanism is implicit in the form of the intensity dependence of the reaction rate (*7*). Photoreactions whose rate depends on $(I_a)^{1/n}$, where $n \geq 1$, include chain reactions for which n is the order of the predominant chain-breaking step with respect to chain carrier. If termination occurs primarily by a reaction that is first order with respect to chain carrying radical, $n = 1$ and the first condition for the existence of a mixing effect is not satisfied. If most chains terminate by radical-radical reaction, $n = 2$ and a mixing effect may occur.

The overall rate of a chain reaction is often directly proportional to the concentration of reactive intermediates. In an optically dense system in the absence of mixing or appreciable diffusion, a nonuniform distribution of intermediates is developed as a result of nonuniform ab-

Richard M. Felder is at Princeton University, Princeton, New Jersey.

* While true for the slab geometry considered by Bhagwat and Dhar, this statement is not true in general. For instance, for a certain region of optical density it is not true for the cylinder, as will be evident later.

sorption of radiation. The observed overall rate is proportional to the mean concentration corresponding to this distribution. The introduction of mixing tends to smooth out these concentration gradients. In the case of radical-radical termination, as will be seen later on, mixing may in principle produce a higher mean concentration and therefore a higher reaction rate. A higher concentration will actually be found in practice and hence a mixing effect will actually be produced, provided the third condition is met. This condition is that the lifetime of the intermediate must be comparable to or longer than a time characteristic of the mixing process. Only under this condition is it possible for the radicals to be mixed and the concentration gradients to be smoothed out.

The lifetime of an individual radical is probably short compared to significant hydrodynamic times. However, in a chain reaction the effective lifetime of the intermediate species is the chain lifetime. This period may be orders of magnitude greater than the lifetime of an individual radical and may equal or exceed the times characteristic of mixing processes.

For ease of interpretation, photochemical and radiation chemical kinetics experiments are, if possible, carried out with optically thin reactant layers in which mixing effects are small. In engineering applications, on the other hand, for purposes of efficiency of radiation source utilization, appreciable radiation attenuation may be demanded. Because of this fact and because chain reactions with radical-radical termination are of industrial interest, it is of value to examine the mixing-kinetics-attenuation interaction in *some* detail.

Noyes and Leighton (*8*) have discussed the effect of the interaction on the interpretation of experimental data. Syrkus (*9*), on the basis of considerations similar to those of Bhagwat and Dhar, has concluded that mixing can significantly increase conversion in radiation chemical reactors. A photobiological process—the growth of algae—is known to be affected by stirring or agitation. Davis (*10*) has reported substantial increases in growth rates upon introduction of mixing in optically dense cultures. Fredrickson and co-workers (*11*) have shown theoretically how mixing, radiation attenuation, and a nonlinear dependence of growth rate on absorbed intensity combine to affect growth rate and efficiency of light utilization in algal growth chambers. The ingredients for the interaction are thus present in algal cultures as well as in chemical chain reactions.

In the present paper the mixing-kinetics-attenuation interaction is examined analytically. Photoreactor equations are formulated for a chain reaction mechanism, and solutions are obtained under the assumptions of stationary concentrations of reaction intermediates throughout the reactor and of low conversion. Parameters include type of chain termination reaction, radiation attenuation mode, reactor geometry, and state of mixing. The conditions for the existence of a mixing effect are examined and the direction of mixing effects is established. Equations are presented for the concentrations of intermediates and final product, and for two types of overall quantum yield. Calculations based on these equations in the case of monochromatic, unidirectional sources are presented graphically and are discussed.

Although the discussion to follow is applicable to reactors for radiation chemical as well as photochemical reactions, it will be presented in the language of photochemistry.

REACTION MECHANISM

A relatively simple chain reaction mechanism is used as the basis for the present study.

$$A \xrightarrow{\phi I_a} R_1 + R_1$$
$$R_1 + B \xrightarrow{k_2} P + R_2$$
$$R_2 + A \xrightarrow{k_3} P + R_1$$
$$R_1 + R_1 \xrightarrow{k_4} A$$
$$R_1 + S \xrightarrow{k_5} P'$$

In the initiation step, reactant A on absorption of radiation is dissociated into two identical radicals R_1. In the propagation reactions, R_1 reacts with a second reactant B to produce a second radical R_2 and stable product P and ultimately R_1 is reproduced. Two chain termination steps are indicated. Homogeneous recombination of the radicals R_1 occurs in one of them. In the other, R_1 disappears via a process that is first order in R_1. S may represent a surface in low-pressure gas phase systems (*7*) or in gaseous systems in turbulent flow (*12*). In either gaseous system first-order termination with respect to R_1 regenerates A; that is, $P' = \frac{1}{2} A + S$. In liquid systems S may represent a scavenger (*13*). One termination step at a time will be considered in the ensuing treatment. It is assumed there is no dark reaction.

Certain halogenation reactions and other types of chain reactions are thought to proceed by the above or closely similar mechanisms. The usual so-called *stationary state kinetics* expressions for the rates and quantum yields of these reactions and of many vinyl polymerizations often have the same form. Thus, for the local rate

$$\frac{dC_P}{dt} = 2k_p \left(\frac{\phi I_a}{k_t}\right)^{1/n} C_B$$

The expression for the local quantum yield is

$$\Phi_a = \frac{2k_p \phi^{1/n} C_B}{k_t^{1/n} I_a^{1-1/n}}$$

In the exponents n is the order of the termination reaction with respect to chain carrier. The factor 2 is specific for the particular mechanism presented above. Otherwise, these expressions show the general dependence of rate and quantum yield on a propagation rate constant, the primary quantum yield, the absorbed intensity, a termination rate constant, and a reactant concentration. The analysis to be presented here will apply not only to the specific mechanism shown above, but also to those reactions whose rates and quantum yields can be represented by expressions of the forms just given.

REACTOR EQUATIONS AND SOLUTIONS

Let us consider a reactor in the form of a cylinder, slab, or annulus as shown in Figure 1. One of the bounding surfaces is a source of radiation that produces a distribution $I_a(\nu, z)$ of volumetric rates of absorption of radiation energy within the reactant.* The reactant is a uniform mixture of the substances A and B. It flows through the reactor with a fully developed velocity distribution $u(\nu)$ and undergoes reaction isothermally under the stimulus of the radiation field in accordance with the mechanism given in the previous section.

Let us calculate the conversion and overall quantum yield of such a reactor, giving special attention to three factors: state of mixing, type of chain termination step, and existence of spatially nonuniform initiation. With re-

* The figure implies absorbed intensity distributions that vary in the ν direction only. Such distributions will be used in calculations to be described later. For the moment we take $I_a = I_a(\nu,z)$.

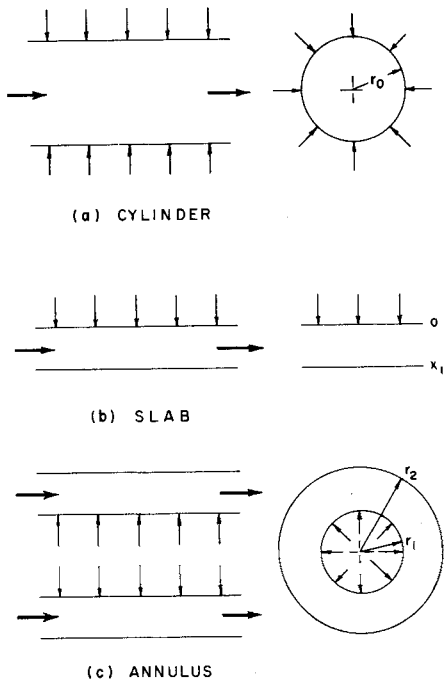

Fig. 1. Photoreactor geometries.

gard to the first of these factors, calculations will be made for three idealized states of mixing: no mixing in any direction, perfect mixing normal to the source but no mixing in the direction of flow, and perfect mixing throughout the reactor.

The calculations are facilitated by the use of two assumptions:

1. The stationary state hypothesis (7) applies. Thus the concentrations of R_1 and R_2 assume steady values immediately on entering the reactor, and they fall to zero immediately on leaving the reactor.

2. Conversion is small. Hence the concentrations of A and B change inappreciably on passing through the reactor.

No Mixing

With these assumptions, material balances for R_1 and R_2 in differential element of reactor volume in the absence of mixing are, respectively

$$2\phi I_a(\nu, z) - k_2 C_B C_{R_1}^{NM}(\nu, z) + k_3 C_A C_{R_2}^{NM}(\nu, z) - 2k_t [C_{R_1}^{NM}(\nu, z)]^n = 0$$

$$k_2 C_B C_{R_1}^{NM}(\nu, z) - k_3 C_A C_{R_2}^{NM}(\nu, z) = 0$$

To conveniently examine the influence of type of termination step, both types are provided for, one at a time, in the first of these equations. In the case of first-order termination with respect to R_1, in the last term of this equation, $n = 1$ and $k_t = \frac{1}{2}k_5 C_S$. For second-order termination, $n = 2$ and $k_t = k_4$.

From these equations one finds

$$\left.\begin{aligned} C_{R_1}^{NM}(\nu, z) &= [\phi I_a(\nu, z)/k_t]^{1/n} \\ C_{R_2}^{NM}(\nu, z) &= \frac{k_2 C_B}{k_3 C_A}[\phi I_a(\nu, z)/k_t]^{1/n} \end{aligned}\right\} \quad (1)$$

These are the expressions for the variation of the concentrations of R_1 and R_2 throughout the reactor in the absence of mixing.

The differential mass balance for the product P is

$$u(\nu)\frac{\partial C_P^{NM}(\nu, z)}{\partial z} = k_2 C_B C_{R_1}^{NM}(\nu, z) + k_3 C_A C_{R_2}^{NM}(\nu, z)$$

As one may see in the mass balance for R_2, the two terms on the right-hand side of the above equation are identical. Therefore we may write this equation as

$$u(\nu)\frac{\partial C_P^{NM}(\nu, z)}{\partial z} = 2k_2 C_B C_{R_1}^{NM}(\nu, z)$$

When this equation is integrated over the reactor length L with $C_P^{NM}(\nu, 0) = 0$, one obtains

$$u(\nu) C_P^{NM}(\nu, L) = 2k_2 C_B \int_0^L C_{R_1}^{NM}(\nu, z)\,dz$$

The mixed average concentration of P in the reactor effluent is by definition

$$\overline{C_P^{NM}(L)} = \frac{1}{\bar{u}S}\int_{\nu_1}^{\nu_2} C_P^{NM}(\nu, L)\,u(\nu)P(\nu)\,d\nu$$

When this and the preceding equation are combined

$$\overline{C_P^{NM}(L)} = 2k_2 C_B \overline{C_{R_1}^{NM}}\,L/\bar{u} \quad (2)$$

where

$$\overline{C_{R_1}^{NM}} = \frac{1}{S}\int_{\nu_1}^{\nu_2}\frac{1}{L}\int_0^L C_{R_1}^{NM}(\nu, z)P(\nu)\,dz\,d\nu \quad (3)$$

Now we derive expressions for two indices of efficiency of source utilization. The first is Φ_0, the overall quantum yield based on incident intensity. The second is Φ_a, the usual overall quantum yield based on absorbed intensity. The amount of chemical change per unit time in terms of product P is $\bar{u}S\,\overline{C_P^{NM}(L)}$ or, expressing $\overline{C_P^{NM}(L)}$ in accordance with Equation (2), the amount of P produced per unit time is $2k_2 C_B \overline{C_{R_1}^{NM}}\,LS$. The total incident radiation per unit time is $I_0 P(\sigma)L$ and the total absorbed radiation per unit time is $\bar{I}_a SL$. Hence

$$\left.\begin{aligned} \Phi_0^{NM} &= \frac{2k_2 C_B \overline{C_{R_1}^{NM}}}{I_0 P(\sigma)/S} \\ \Phi_a^{NM} &= \frac{2k_2 C_B \overline{C_{R_2}^{NM}}}{\bar{I}_a} \end{aligned}\right\} \quad (4)$$

Perfect Lateral Mixing, No Axial Mixing

In the case of perfect mixing normal to the source, all concentrations are uniform in that direction, and the effective rate of photoinitiation at each axial position can be shown to be that corresponding to the mean rate of radiation absorption at that position. A treatment similar to that above leads to the following equations. The concentrations of the intermediates are given by

$$\left.\begin{aligned} C_{R_1}^{PM}(z) &= [\phi \bar{I}_a(z)/k_t]^{1/n} \\ C_{R_2}^{PM}(z) &= \frac{k_2 C_B}{k_3 C_A}[\phi \bar{I}_a(z)/k_t]^{1/n} \end{aligned}\right\} \quad (5)$$

where

$$\bar{I}_a(z) = \frac{1}{S}\int_{\nu_1}^{\nu_2} I_a(\nu, z)P(\nu)d\nu \tag{6}$$

The effluent product concentration is

$$C_P^{PM}(L) = 2k_2C_BC_{R_1}^{PM}L/\bar{u}$$

where

$$\overline{C_{R_1}^{PM}} = \frac{1}{L}\int_0^L C_{R_1}^{PM}(z)dz \tag{7}$$

and the quantum yields are

$$\left.\begin{aligned}\Phi_p^{PM} &= \frac{2k_2C_BC_{R_1}^{PM}}{I_0P(\sigma)/S}\\ \Phi_a^{PM} &= \frac{2k_2C_BC_{R_1}^{PM}}{\bar{I}_a}\end{aligned}\right\} \tag{8}$$

Perfect Mixing Throughout Reactor

Concentrations of all substances are uniform throughout the reactor and the effective initiation rate is given by the volume-averaged rate of absorption of radiation energy. In formulating the applicable mass balances, the rates of disappearance of R_1 and R_2 via outflow from the reactor are assumed to be negligibly small, as they normally will be. Expressions obtained for this case are

$$\left.\begin{aligned}C_{R_1}^* &= \left(\frac{\phi\bar{I}_a}{k_t}\right)^{1/n}\\ C_{R_2}^* &= \frac{k_2C_B}{k_3C_A}\left(\frac{\phi\bar{I}_a}{k_t}\right)^{1/n}\end{aligned}\right\} \tag{9}$$

where

$$\bar{I}_a = \frac{1}{L}\int_0^L \frac{1}{S}\int_{\nu_1}^{\nu_2} I_a(\nu, z)P(\nu)d\nu dz \tag{10}$$

$$C_P^* = 2k_2C_BC_{R_1}^*V/F \tag{11}$$

$$\left.\begin{aligned}\Phi_p^* &= \frac{2k_2C_BC_{R_1}^*}{I_0P(\sigma)/S}\\ \Phi_a^* &= \frac{2k_2C_BC_{R_1}^*}{\bar{I}_a}\end{aligned}\right\} \tag{12}$$

For each mixing state one sees that the product concentration and quantum yields vary linearly with an appropriate average concentration of R_1. Hence, in assessing the effect of mixing on these quantities, one may focus attention on the variation with mixing of the average concentration of R_1.

THE EFFECTS OF MIXING

If we combine Equations (1) and (3), and (5), (6), and (7), and (9) and (10), we obtain the following expressions for the concentrations of R_1 in the three mixing states:

$$\overline{C_{R_1}^{NM}} = \frac{1}{L}\int_0^L \frac{1}{S}\int_{\nu_1}^{\nu_2} [\phi I_a(\nu, z)/k_t]^{1/n}P(\nu)d\nu dz$$

$$\overline{C_{R_1}^{PM}} = \frac{1}{L}\int_0^L \left\{\phi\left[\frac{1}{S}\int_{\nu_1}^{\nu_2} I_a(\nu, z)P(\nu)d\nu\right] \Big/ k_t\right\}^{1/n} dz$$

$$C_{R_1}^* = \left\{\phi\left[\frac{1}{L}\int_0^L \frac{1}{S}\int_{\nu_1}^{\nu_2} I_a(\nu, z)P(\nu)d\nu dz\right] \Big/ k\right\}^{1/n}$$

In these equations may be found formal statements of the conditions required for the existence of mixing effects and on the direction of mixing effects.

First of all, for $n = 1$, we see that all three concentrations are identical and no mixing effect exists.

For $n = 2$, inspection of the expressions for the radical concentrations shows that generally these concentrations will be different and that mixing effects may exist. In order to facilitate determination of the direction of mixing effects in the presence of second-order termination, let us recall the Schwarz inequality (*14*)

$$\int_{\nu_1}^{\nu_2} f(\nu, z)g(\nu, z)d\nu \leq \left\{\int_{\nu_1}^{\nu_2} [f(\nu, z)]^2 d\nu \int_{\nu_1}^{\nu_2} [g(\nu, z)]^2 d\nu\right\}^{1/2}$$

where $f(\nu, z)$ and $g(\nu, z)$ are any functions that are at least piecewise continuous over the intervals $\nu_1 \leq \nu \leq \nu_2$ and $0 \leq z \leq L$. Let us first use this expression to establish the relative magnitudes of $\overline{C_{R_1}^{NM}}$ and $\overline{C_{R_1}^{PM}}$. For this purpose we choose $f(\nu, z)$ and $g(\nu, z)$ to be

$$f(\nu, z) = [I_a(\nu, z)P(\nu)]^{1/2}$$

$$g(\nu, z) = \frac{1}{S}[\phi P(\nu)/k_4]^{1/2}$$

With these definitions one finds that the Schwarz inequality states

$$\frac{1}{S}\int_{\nu_1}^{\nu_2} [\phi I_a(\nu, z)/k_4]^{1/2}P(\nu)d\nu \leq \left\{\phi\left[\frac{1}{S}\int_{\nu_1}^{\nu_2} I_a(\nu, z)P(\nu)d\nu\right] \Big/ k_4\right\}^{1/2}$$

These quantities are the integrands of the integrals with respect to z in the expressions for $\overline{C_{R_1}^{NM}}$ and $\overline{C_{R_1}^{PM}}$. The inequality is valid at each value of z from 0 to L, and it is therefore valid for the integral with respect to z over this interval. Hence

$$\overline{C_{R_1}^{NM}} \leq \overline{C_{R_1}^{PM}}$$

In establishing the relative magnitudes of $\overline{C_{R_1}^{PM}}$ and $C_{R_1}^*$, we take the integrals in the inequality with respect to z instead of ν, and $f(\nu, z)$ and $g(\nu, z)$ are taken as

$$f(\nu, z) = \left[\int_{\nu_1}^{\nu_2} I_a(\nu, z)P(\nu)d\nu\right]^{1/2}$$

$$g(\nu, z) = \frac{1}{L}(\phi/Sk_4)^{1/2}$$

The resulting inequality is

$$\frac{1}{L}\int_0^L \left\{\phi\left[\frac{1}{S}\int_{\nu_1}^{\nu_2} I_a(\nu, z)P(\nu)d\nu\right] \Big/ k_4\right\}^{1/2} dz \leq \left\{\phi\left[\frac{1}{L}\int_0^L \frac{1}{S}\int_{\nu_1}^{\nu_2} I_a(\nu, z)P(\nu)d\nu dz\right] \Big/ k_4\right\}^{1/2}$$

or

$$\overline{C_{R_1}^{PM}} \leq C_{R_1}^*$$

On examination of the expressions for $\overline{C_{R_1}^{NM}}$, $\overline{C_{R_1}^{PM}}$, and $C_{R_1}^*$, one finds that in the above inequalities, the *equal* signs apply when $I_a(\nu, z)$ is essentially a constant, that is, for weak absorption or attenuation. The *inequality* signs apply in the presence of appreciable absorption or attenuation. Thus attenuation is required in order to have an effect.

TABLE 1. GEOMETRICAL QUANTITIES

Quantity	Geometry: Cylinder	Slab	Annulus
$\nu_1 \leq \nu \leq \nu_2$, normal coordinate and its range	$0 \leq r \leq r_o$	$0 \leq x \leq x_1$	$r_1 \leq r \leq r_2$
σ, source location along ν coordinate	r_o	0	r_1
b, reactor thickness	$2r_o$	x_1	$r_2 - r_1$
ρ, dimensionless normal coordinate, $0 \leq \rho \leq 1$	r/r_o	x/x_1	$\dfrac{r - r_1}{r_2 - r_1}$
$\bar{R}$, average dimensionless radius	1/4	1	$\dfrac{r_1 + r_2}{2r_1}$
S, flow cross-sectional area	πr_o^2	wx_1	$\pi(r_2^2 - r_1^2)$
$P(\sigma)$, source perimeter	$2\pi r_o$	w	$2\pi r_1$

We have now shown for $n = 2$ with no significant limitation on the form of $I_a(\nu,z)$ that in the presence of spatially nonuniform absorption, and apart from considerations of relative chemical and mixing time scales, the introduction of mixing will result in an increase in the mean concentration of intermediate and hence in conversion and overall quantum yields. The introduction of lateral mixing alone where there was previously no mixing in any direction will produce a certain increase in performance. The further introduction of axial mixing will produce a further increase in performance.*

The increase in magnitude of intermediate concentration upon introduction of one or the other idealized state of perfect mixing is the maximum change that may be realized and will be realized when the chain lifetime is long compared to the time of the mixing process. Shorter chain lifetimes will lead to less than the maximum effect or, for sufficiently short lifetimes, to no effect at all.

Statements are occasionally found in the literature (*1*, 3) that assert that improvements in photoreactor performance brought about by turbulence or mixing occur because of the resultant exposure to the light near the source of reactant that would otherwise have remained in the dark. In terms of the present interpretation, increased exposure of reactant to the light produces no effect in the case of first-order termination, and with radical-radical termination the improvement comes about because of increased average concentration of chain carrier.

CALCULATED RESULTS USING IDEALIZED SOURCES

In this section the equations developed above are used to calculate results for specific reactor geometries, attenuation modes, and types of termination reaction. The reactor-source configurations treated are those shown in Figure 1.† All bounding surfaces are taken to be nonreflecting. The sources are monochromatic, of uniform intensity over their entire surface, and emit radiation only in the direction normal to the source surface. Such sources are highly idealized. Results of calculations based on them are approximations to the results corresponding to real sources.

Quantities associated with the reactor geometries of interest are presented in Table 1. The reactor thickness b is used as the path length in the definition of the reactor optical thickness τ described below. The definition of an average dimensionless radius permits retention of generality in the formulas for the different geometries and attenuation modes.‡

Two attenuation or absorption modes are treated: the exponential mode and the constant energy loss mode. Radiations for which the volumetric rate of absorption of radiation energy decreases exponentially with distance from the source include, in varying degrees of approxi-

* The preceding discussion on conditions under which effects of mixing may be found and on the direction of mixing effects was formulated in terms of *photo*initiation. It should be pointed out that it applies for other forms of initiation as well, for example, *thermal* initiation. In this case we replace $\phi I_a(\nu,z)$ with $k_i C_I(\nu,z)$. Thus in an isothermal system in the absence of mixing, the thermal dissociation of an initiator, I, spatially nonuniformly distributed, will proceed at a local rate $k_i C_I(\nu,z)$, and the mean concentration of intermediate whose magnitude is associated with the mixing state is linearly related to the average of the $(1/n)$th root of $k_i C_I(\nu,z)$. When the same quantity of initiator is uniformly distributed with respect to the ν coordinate or with respect to both the ν and z coordinates, the concentrations of intermediate of interest will be those corresponding to the $(1/n)$th roots of the averages of $k_i C_I(\nu,z)$ over one or both of the coordinates, respectively.

† The slab is of infinite width. Calculations are based on a width w.

‡ With regard to the mean dimensionless radius of the cylinder the factor ¼ is found to arise naturally in all of the expressions for this geometry, and the generalized formulas referred to become possible if we define $\bar{R} = ¼$ for this geometry. No physical meaning is attached to the definition.

TABLE 2. EXPONENTIAL ATTENUATION QUANTITIES

Quantity	Geometry: Cylinder	Slab	Annulus
τ	$2\mu r_o$	μx_1	$\mu(r_2 - r_1)$
β	—	∞	μr_1
$p(\tau)$	$1 + e^{-\tau}$	1	1
$q(\tau)$	$1 + e^{-\tau}$	$1 - e^{-\tau}$	$1 - e^{-\tau}$
$I_a(\nu)$	$\mu I_o \dfrac{r_o}{r}\left[e^{-\mu(r_o+r)} + e^{-\mu(r_o-r)}\right]$	$\mu I_o e^{-\mu x}$	$\mu I_o \dfrac{r_1}{r} e^{-\mu(r-r_1)}$
$\bar{I}_a$	$\mu I_o q(\tau)/(\bar{R}\tau)$	$\mu I_o q(\tau)/(\bar{R}\tau)$	$\mu I_o q(\tau)/(\bar{R}\tau)$
$\overline{C_{R_1}^{NM}}/(\phi\mu I_o/k_t)^{1/n}$	$\displaystyle\int_0^1 \left(\frac{2}{\rho} e^{-\tau/2} \cosh\frac{\tau\rho}{2}\right)^{1/n} 2\rho d\rho$	$\displaystyle\int_0^1 \left(e^{-\tau\rho}\right)^{1/n} d\rho$	$\displaystyle\frac{1}{\bar{R}}\int_0^1 \left[\frac{e^{-\tau\rho}}{1 + 2(\bar{R} - 1)\rho}\right]^{1/n} [1 + 2(\bar{R} - 1)\rho] d\rho$
$\overline{C_{R_1}^{PM}}/(\phi\mu I_o/k_t)^{1/n}$	$\left[\dfrac{1}{\bar{R}} e^{-\tau/2} \displaystyle\int_0^1 \left(\cosh\frac{\tau\rho}{2}\right) d\rho\right]^{1/n}$	$\left[\displaystyle\int_0^1 e^{-\tau\rho} d\rho\right]^{1/n}$	$\left[\dfrac{1}{\bar{R}}\displaystyle\int_0^1 e^{-\tau\rho} d\rho\right]^{1/n}$

mation, visible and ultraviolet light, x-rays, and gamma rays and beta particles from isotopic sources. In the constant energy loss mode, the volumetric absorption rate is constant with distance from the source up to a point known as the range, at which point the absorption falls to zero. Constant energy loss radiation is an approximation to those associated with heavy particles, such as alpha particles, heavy ions, and fission fragments. Constant energy loss radiation has its analogy in certain situations of use of weakly absorbed visible or ultraviolet light. When the reaction mixture is only partly illuminated, the illuminated region corresponds to the region of constant energy loss within the particle range and the dark region to the zone outside the particle range. Diffusion effects in partially illuminated reaction vessels in which a nonchain photochemical reaction occurred have been discussed by Hill (*15*) and by Pritchard and Pritchard (*16*).

In Tables 2 and 3 quantities peculiar to the two attenuation modes are given. The optical thickness τ is based on the reactor thickness b of Table 1, and is measured in units of $1/\mu$, the radiation mean free path. For Beer's law absorption, $\mu = \alpha C_A$. For heavy particles, $1/\mu = R$, the particle range. Otherwise μ is taken to be the linear absorption coefficient for the radiation in question. A quantity that is useful in describing the annular reactor is β, the radius of the source measured in units of the mean free path. For the slab, $\beta = \infty$. It is not defined for the cylinder.

A number of the quantities in Table 3 are expressed by different relations in different regions of the parameter τ. Thus for heavy particle radiation, the region $\tau \leq 1$ corresponds to a particle range greater than the reactor thickness. The region $\tau > 1$ corresponds relatively to smaller ranges. In the case of the cylinder and heavy particle radiation the region $\tau > 1$ is itself divided. For $1 \leq \tau \leq 2$, the range lies between the radius and the diameter of the cylinder, and for $\tau > 2$, the range is less than the cylinder radius.

The functions $p(\tau)$ and $q(\tau)$ are used to permit retention of generality in formulas used in this section.

Expressions for $I_a(\nu)$, the absorbed intensity distribution, are also given in Tables 2 and 3. The expression for exponential attenuation in the slab is well known. Schechter and Wissler (*17*) have presented without derivation the expression for the distribution of intensity of exponentially attenuated radiation in the cylindrical reactor. Huff and Walker (*12*) have derived the expression for the corresponding absorbed intensity distribution. Each of the expressions for $I_a(\nu)$ can be derived by a method that is illustrated in the Appendix.* The method is similar to that of Huff and Walker.

$\overline{I_a}$ is the average absorbed intensity. It can be represented by a single expression that is valid for both attenuation modes and all three geometries.

Because the absorbed intensity distributions for the sources of interest vary in the ν direction only and not in the z direction as well, two of the states of mixing treated in the previous section become identical for present purposes. Those two are the state of perfect lateral mixing with no axial mixing, and the state of perfect mixing throughout the reactor. Thus the simultaneous introduction of lateral and axial mixing produces no effect beyond that resulting from the introduction of lateral mixing alone. Therefore in this section two states of mixing are treated and these are referred to as the states of no mixing and of perfect mixing. In the latter instance the mixing is in the lateral direction.

* Deposited as document 8514 with the American Documentation Institute, Photoduplication Service, Library of Congress, Washington 25, D. C., and may be obtained for $2.50 for photoprints or $1.75 for 35-mm. microfilm.

Equations Used for Calculations

It is convenient to deal with the mixed-average effluent product concentration and the quantum yields as dimensionless quantities. Two such forms of expressions for these quantities have been found to be useful. We derive them first and indicate their utility subsequently.

For the effluent product concentration, in the case of no mixing, we divide both sides of Equation (2) by $2k_2C_B(\phi\mu I_o/k_t)^{1/n}L/\overline{u}$, thereby obtaining

$$\overline{C_P^{NM}}(L)/[2k_2C_B(\phi\mu I_o/k_t)^{1/n}L/\overline{u}] = \overline{C_{R_1}^{NM}}/(\phi\mu I_o/k_t)^{1/n} \tag{13}$$

For the quantum yields for the no mixing case, Equations (4) may be written

$$\Phi_o^{NM} = \frac{2k_2C_B(\phi\mu I_o/k_t)^{1/n}}{I_oP(\sigma)/S}\left[\frac{\overline{C_{R_1}^{NM}}}{(\phi\mu I_o/k_t)^{1/n}}\right]$$

$$\Phi_a^{NM} = \frac{2k_2C_B(\phi\mu I_o/k_t)^{1/n}}{\overline{I_a}}\left[\frac{\overline{C_{R_1}^{NM}}}{(\phi\mu I_o/k_t)^{1/n}}\right]$$

If we substitute for $\overline{I_a}$, $P(\sigma)$, and S using the expressions for these quantities given in Tables 1 to 3, it will be found that the above relations can be rearranged to give

$$\left.\begin{aligned}\Phi_o^{NM}/[2k_2C_B\phi^{1/n}/k_t^{1/n}(\mu I_o)^{1-1/n}]\;\overline{\qquad} &= \overline{R\tau}[\overline{C_{R_1}^{NM}}/(\phi\mu I_o/k_t)^{1/n}]\\ \Phi_a^{NM}/[2k_2C_B\phi^{1/n}/k_t^{1/n}(\mu I_o)^{1-1/n}]\;\overline{\qquad} &= [\overline{R\tau}/q(\tau)][\overline{C_{R_1}^{NM}}/(\phi\mu I_o/k_t)^{1/n}]\end{aligned}\right\} \tag{14}$$

The corresponding equations for perfect mixing are obtained by replacing $\overline{C_{R_1}^{NM}}$ by $\overline{C_{R_1}^{PM}}$ in Equations (13) and (14).

Equations (13) and (14) constitute one of the two desired forms of dimensionless representation. The other is derived from them by first replacing μ in the left-hand sides by its equivalent τ/b. Then both sides of Equation (13) are multiplied by $\tau^{1/n}$ and both sides of Equation (14) are divided by $\tau^{1-1/n}$. There are thus obtained, again for the no mixing case

$$\overline{C_P^{NM}}(L)/[2k_2C_B(\phi I_o/bk_t)^{1/n}L/\overline{u}]\;\overline{\qquad} = \tau^{1/n}[\overline{C_{R_1}^{NM}}/(\phi\mu I_o/k_t)^{1/n}] \tag{15}$$

$$\left.\begin{aligned}\Phi_a^{NM}/[2k_2C_B\phi^{1/n}/k_t^{1/n}(I_o/b)^{1-1/n}]\;\underline{\qquad} &= \overline{R\tau}^{1/n}[\overline{C_{R_1}^{NM}}/(\phi\mu I_o/k_t)^{1/n}]\\ \Phi_o^{NM}/[2k_2C_B\phi^{1/n}/k_t^{1/n}(I_o/b)^{1-1/n}]\;\underline{\qquad} &= [\overline{R\tau}^{1/n}/q(\tau)][\overline{C_{R_1}^{NM}}/(\phi\mu I_o/k_t)^{1/n}]\end{aligned}\right\} \tag{16}$$

The right-hand sides of Equations (13) to (16) in both the no mixing and perfect mixing cases can be shown to be functions of reactor optical thickness τ with reactor geometry, attenuation mode, and n as parameters. Therefore the equations are represented graphically in plots of the left-hand sides vs. τ. The left-hand sides, however, contain one or the other of the ingredients of τ, either μ or b. For convenience in visualizing the effects of varying, say,

TABLE 3. CONSTANT ENERGY LOSS ATTENUATION QUANTITIES

Quantity	Geometry: Cylinder	Slab	Annulus
τ	$2\mu r_o$	μx_1	$\mu(r_2 - r_1)$
β	—	∞	μr_1
$p(\tau)$	$2,\ 0 \leq \tau \leq 1$ $1,\ \tau > 1$	1	1
$q(\tau)$	$\tau,\ \tau \leq 1$ $1,\ \tau > 1$	$\tau,\ \tau \leq 1$ $1,\ \tau > 1$	
$I_a(\nu)$	$2\mu I_o \frac{r_o}{r},\ 0 \leq \rho \leq 1,\ 0 \leq \tau \leq 1$	$\mu I_o,\ 0 \leq \rho \leq 1,\ \tau \leq 1$	$\mu I_o \frac{r_1}{r},\ 0 \leq \rho \leq 1,\ \tau \leq 1$
	$2\mu I_o \frac{r_o}{r},\ 0 \leq \rho \leq \frac{2}{\tau} - 1$ $\mu I_o \frac{r_o}{r},\ \frac{2}{\tau} - 1 \leq \rho \leq 1$ $\Big\}\ 1 \leq \tau \leq 2$	$\mu I_o,\ 0 \leq \rho \leq \frac{1}{\tau}$ $0,\ \frac{1}{\tau} \leq \rho \leq 1$ $\Big\}\ \tau > 1$	$\mu I_o \frac{r_1}{r},\ 0 \leq \rho \leq \frac{1}{\tau}$ $0,\ \frac{1}{\tau} \leq \rho \leq 1$ $\Big\}\ \tau > 1$
	$0,\ 0 \leq \rho \leq \frac{2}{\tau} - 1$ $\mu I_o \frac{r_o}{r},\ \frac{2}{\tau} - 1 \leq \rho \leq 1$ $\Big\}\ \tau \geq 2$		
$\bar{I}_a$	$\mu I_o q(\tau)/(\bar{R}\tau)$	$\mu I_o q(\tau)/(\bar{R}\tau)$	$\mu I_o q(\tau)/(\bar{R}\tau)$
$\overline{C_{R_1}^{NM}}/(\phi\mu I_o/k_t)^{1/n}$	$2\int_0^1 (2/\rho)^{1/n}\rho d\rho,\ 0 \leq \tau \leq 1$	$\int_0^1 (1)^{1/n} d\rho,\ \tau \leq 1$	$\frac{1}{\bar{R}}\int_0^1 \left[\frac{1}{1 + 2(\bar{R}-1)\rho}\right]^{1/n} [1 + 2(\bar{R}-1)\rho] d\rho,\ \tau \leq 1$
	$2\int_0^{(2/\tau)-1} (2/\rho)^{1/n}\rho d\rho + 2\int_{(2/\tau)-1}^1 (1/\rho)^{1/n}\rho d\rho,\ 1 \leq \tau \leq 2$	$\int_0^{1/\tau} (1)^{1/n} d\rho,\ \tau > 1$	$\frac{1}{\bar{R}}\int_0^{1/\tau} \left[\frac{1}{1 + 2(\bar{R}-1)\rho}\right]^{1/n} [1 + 2(\bar{R}-1)\rho] d\rho,\ \tau > 1$
	$2\int_{1-(2/\tau)}^1 (1/\rho)^{1/n}\rho d\rho,\ \tau \geq 2$		
$\overline{C_{R_1}^{PM}}/(\phi\mu I_o/k_t)^{1/n}$	$\left[2\int_0^1 2 d\rho\right]^{1/n},\ 0 \leq \tau \leq 1$	$\left[\int_0^1 1 \cdot d\rho\right]^{1/n},\ \tau \leq 1$	$\left[\frac{1}{\bar{R}}\int_0^1 1 \cdot d\rho\right]^{1/n},\ \tau \leq 1$
	$\left[2\int_0^{(2/\tau)-1} 2 d\rho + 2\int_{(2/\tau)-1}^1 1 \cdot d\rho\right]^{1/n},\ 1 \leq \tau \leq 2$	$\left[\int_0^{1/\tau} 1 \cdot d\rho\right]^{1/n},\ \tau > 1$	$\left[\frac{1}{\bar{R}}\int_0^{1/\tau} 1 \cdot d\rho\right]^{1/n},\ \tau > 1$
	$\left[2\int_{1-(2/\tau)}^1 1 \cdot d\rho\right]^{1/n},\ \tau \geq 2$		

μ while b is held constant, and vice versa, the two dimensionless forms are used. In Equations (13) and (14), μ appears in the left-hand sides. Therefore in these equations variation in τ is assumed to be due to variation in b at constant μ, and plots of Equations (13) and (14) are labelled $\tau = \tau(b)$. In Equations (15) and (16), b appears on the left. Hence variation in τ here is visualized as arising through variation in μ at constant b. Plots of Equations (15) and (16) are labelled $\tau = \tau(\mu)$.

For the annulus, $\beta = \mu r_1$ is a parameter in the use of Equations (13) and 14). The response to variation in reactor thickness is thus obtained at constant source size as well as at constant absorption coefficient. In the use of Equations (15) and (16) for this same geometry, the parameter is r_2/r_1.*

As one can see in Equations (13) to (16), when written for both extreme states of mixing, the dimensionless mixed average effluent product concentration and overall quantum yields are linearly related to the ratio of an average concentration of R_1 to the concentration expressed by $(\phi\mu I_o/k_t)^{1/n}$. These dimensionless concentrations may be evaluated by using Equations (1), (3), (5), (6), and (7), leading to

$$\overline{C}_{R_1}^{NM}/(\phi\mu I_o/k_t)^{1/n} = \frac{1}{S}\int_{\nu_1}^{\nu_2} [p(\tau)I_a(\nu)/I_a(\sigma)]^{1/n}P(\nu)d\nu$$

$$\overline{C}_{R_1}^{PM}/(\phi\mu I_o/k_t)^{1/n} = \left\{\frac{1}{S}\int_{\nu_1}^{\nu_2} [p(\tau)I_a(\nu)/I_a(\sigma)]P(\nu)d\nu\right\}^{1/n}$$

* In formulas involving the annulus when r_2/r_1 is the desired parameter, it is introduced by replacing $\bar{R}$ by its equivalent, $(1/2)[(r_2/r_1) + 1]$. Similarly, when β is the parameter, it is introduced through the relation $\bar{R} = (\tau + 2\beta)/2\beta$.

After substituting in these equations the expressions for $p(\tau)$, absorbed intensity, and geometrical quantities given in Tables 1 to 3, one can obtain the expressions given in Tables 2 and 3 for the dimensionless concentrations. Expressions for these concentrations that were used in calculations were obtained after evaluation of the integrals in Tables 2 and 3. The final expressions for all combinations of parameters are shown in Table 4. The expressions for exponential attenuation in the cylinder and the annulus were evaluated with a high-speed digital computer.

Calculations of overall quantum yield were made only for the yield based on incident intensity. This yield differs from the yield based on absorbed intensity only by the factor $q(\tau)$. Since $q(\tau)$ is unity at sufficiently large τ, the two yields are identical there and are different only at small τ. Φ_o is, of course, of more direct engineering interest than Φ_a, the former being a more direct measure of efficiency of source utilization.

First-Order Termination

For first-order termination, as one can see in Table 4, the dimensionless concentration of R_1 can be represented by a single generalized expression that is valid for both attenuation modes and all three geometries. Dimensionless effluent product concentrations and overall quantum yields were calculated using the expression in Table 4 and Equations (13) to (16). The results are shown in Figures 2 to 4. Since for $n = 1$ there is no effect of mixing, each of the curves in these figures is valid for both extreme states of mixing.

TABLE 4. DIMENSIONLESS CONCENTRATIONS OF R_1

Main body of table contains expressions for $\overline{C}_{R_1}/(\phi\mu I_o/k_t)^{1/n}$

Attenuation mode	State of mixing	Geometry: Cylinder	Slab	Annulus
			$n = 1$	
Exp	*NM*, *PM*	$\dfrac{q(\tau)}{\bar{R}\tau}$	$\dfrac{q(\tau)}{\bar{R}\tau}$	$\dfrac{q(\tau)}{\bar{R}\tau}$
C.E.L.	*NM*, *PM*			
			$n = 2$	
Exp	*NM*	$2(2e^{-\tau/2})^{1/2}\int_0^1 [\rho\cosh(\tau\rho/2)]^{1/2}d\rho$	$\dfrac{1-e^{-\tau/2}}{\tau/2}$	I_1*
	PM	$\left[\dfrac{q(\tau)}{\bar{R}\tau}\right]^{1/2}$	$\left[\dfrac{q(\tau)}{\bar{R}\tau}\right]^{1/2}$	$\left[\dfrac{q(\tau)}{\bar{R}\tau}\right]^{1/2}$
		$\dfrac{4}{3}2^{1/2}, 0 \leqq \tau \leqq 1$	$1, \tau \leqq 1$	$[(2\bar{R}-1)^{3/2}-1]/[3\bar{R}(\bar{R}-1)], \tau \leqq 1$
	NM	$\dfrac{4}{3}\left[1-\left(2^{1/2}-1\right)\left(1-\dfrac{2}{\tau}\right)^{3/2}\right], 1 \leqq \tau \leqq 2$	$\dfrac{1}{\tau}, \tau > 1$	$\left\{\left[\dfrac{2(\bar{R}-1)}{\tau}+1\right]^{3/2}-1\right\}\Big/$
C.E.L.		$\dfrac{4}{3}\left[1-\left(1-\dfrac{2}{\tau}\right)^{3/2}\right], \tau \geqq 2$		$[3\bar{R}(\bar{R}-1)], \tau > 1$
	PM	$\left[\dfrac{q(\tau)}{\bar{R}\tau}\right]^{1/2}$	$\left[\dfrac{q(\tau)}{\bar{R}\tau}\right]^{1/2}$	$\left[\dfrac{q(\tau)}{\bar{R}\tau}\right]^{1/2}$

* $I_1 = \dfrac{2}{\bar{R}\tau}\left\{1-(2\bar{R}-1)^{1/2}e^{-\tau/2}-\dfrac{\pi^{1/2}e^{\tau[(\bar{R}-1)]}}{2\left[\dfrac{\tau}{4(\bar{R}-1)}\right]^{1/2}}\left[\mathrm{erf}\left(\dfrac{\tau}{4(\bar{R}-1)}\right)^{1/2}-\mathrm{erf}\left(\dfrac{2\bar{R}-1}{4(\bar{R}-1)}\tau\right)^{1/2}\right]\right\}$

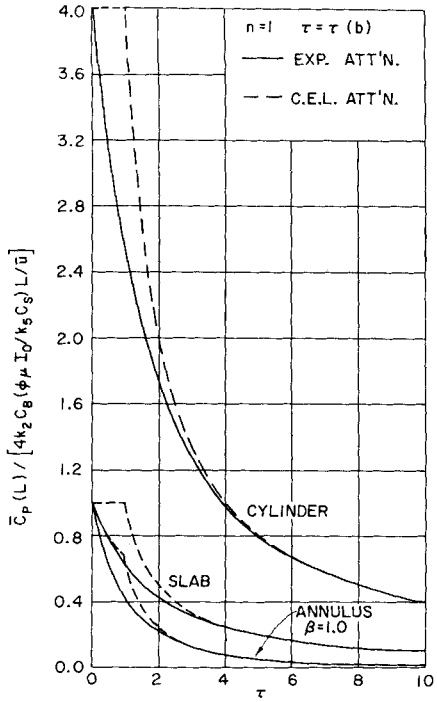

Fig. 2. Dimensionless mixed average effluent product concentration. Variation with b at constant μ [$\tau = \tau(b)$]. $n = 1$.

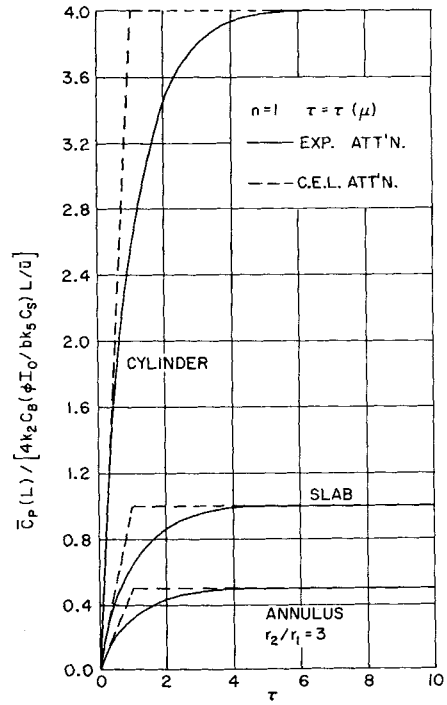

Fig. 3. Dimensionless mixed average effluent product concentration. Variation with μ at constant b [$\tau = \tau(\mu)$]. $n = 1$.

In Figure 2, the dependence of dimensionless product concentration on reactor thickness is shown for the two attenuation modes and three geometries. At small thicknesses the source radiation is not completely absorbed. At sufficiently large thicknesses ($\tau > 1$ for constant energy loss radiation), absorption is complete or essentially so. Generally the product concentration decreases with increasing reactor thickness (except for $\tau < 1$ for the cylinder and the slab with constant energy loss radiation), the dilution effect predominating over any additional absorption. At a given thickness, the concentration decreases in the order, cylinder, slab, and annulus. This is the order of decreasing source surface area-to-reactant volume ratio. The limiting dimensionless concentrations as $\tau \to 0$, as well as those at large τ, are identical for the two attenuation modes and the same geometry. Identical concentrations are found because the expressions for $\overline{I_a}$, to which the concentrations are proportional, become identical for the two modes with very weak and very strong absorption (see the expressions for $\overline{I_a}$ in Tables 2 and 3).

The variation of dimensionless product concentration with absorption coefficient is shown in Figure 3. At zero absorption coefficient there is no absorption of radiation and no product produced. As the absorption coefficient increases from zero, the product concentration increases, and when absorption is complete the product concentration reaches a limiting value.

For $n = 1$, Equations (14) and (16) become identical, and the quantum yields are functions solely of τ and not of the separate ingredients of τ, μ and b. The relations for the yield based on incident intensity are shown in Figure 4. No dependence on geometry is found. All reactors are equally efficient at the same optical thickness. The same limiting efficiency is approached for both attenuation modes as τ becomes large, that is, when absorption becomes complete.

Second-Order Termination

The expressions for the dimensionless concentrations of R_1 for $n = 2$ for all combinations of parameters are shown in Table 4. For perfect mixing, a single generalized expression is valid for both attenuation modes and all three geometries; it is simply the square root of the expression for $n = 1$. The expressions applying in the case of no mixing are in general more complicated and are unique for each combination of geometry and attenuation mode.

We have seen earlier that for radical-radical termination in the presence of radiation attenuation and suitable chemical and mixing time scales, the introduction of mixing will lead to increased intermediate concentration and hence to increased conversion and overall quantum yield. The increase will be maximized if the chemical time scale is long compared to the mixing time scale. Through the use of the expressions in Table 4, we may calculate a measure of the maximum relative effect of mixing, namely, the ratio, $\overline{C_{R_1}^{PM}}/\overline{C_{R_1}^{NM}}$. The results of such calculations are presented in Figures 5 and 6. Figure 5 is for exponential attenuation, and Figure 6, for constant energy loss attenuation. In both figures it is seen that, with few exceptions, the introduction of mixing always leads to an

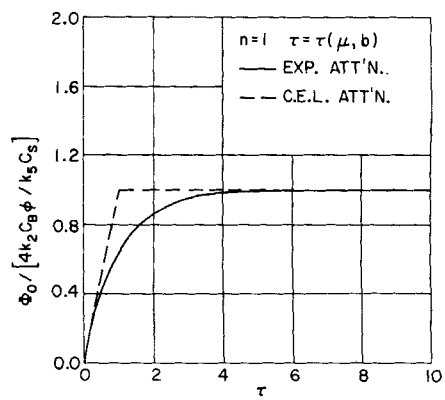

Fig. 4. Dimensionless overall quantum yield based on incident intensity. $n = 1$.

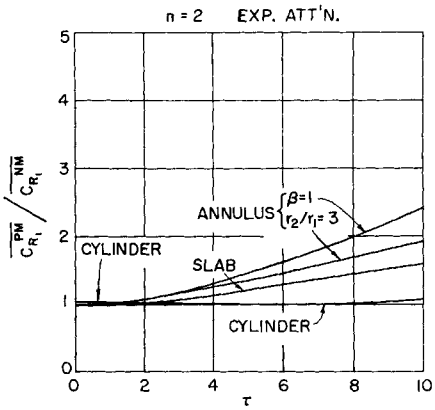

Fig. 5. Maximum effect of mixing, exponential attenuation.

increase in intermediate concentration. The exceptions involve the slab and the annulus in the limit as $\tau \to 0$ for exponential attenuation, and the region for which $\tau \leq 1$ for constant energy loss attenuation. In these cases there is no attenuation and hence no mixing effect. There is a positive, though sometimes very small, effect of mixing in the cylinder at all values of τ, including $\tau \to 0$. Thus even for optically thin cylindrical reactors there is a nonuniform distribution of initiation rates, the rate approaching infinity as $\tau \to 0$ [see the expression for $I_a(\nu)$ in Tables 2 and 3]. At sufficiently large τ for all geometries and both attenuation modes the ratio $C_{R_1}^{PM}/C_{R_1}^{NM}$ increases with τ in the order cylinder, slab, and annulus, and in the order exponential attenuation, constant energy loss attenuation. A monotonic increase in the ratio with τ for the cylinder is not found until $\tau > \sim 6$ for exponential attenuation, and until $\tau > 2$ for constant energy loss attenuation, that is, until absorption is complete or virtually so, and radiant rays or particles from opposite ends of a diameter no longer overlap.

In Figures 5 and 6 one may find the values of τ at which a maximum increase in intermediate concentration, and hence of conversion and quantum yield, of a certain percentage results from the transition from no mixing to perfect mixing. Values of τ corresponding to 1, 10, and 100% maximum increases are given in Table 5. The significance of the results given there is better appreciated when one considers the magnitudes of $1/\mu$, the mean free paths of various radiations of interest (5, 22 to 25). These range widely. For instance, in water they are approximately 20 μ for U-235 fission fragments, 40 μ for Po-210 alpha particles, 0.1 cm. for Sr-90 beta particles, and 16 cm. for Co-60 gamma rays. In air at atmospheric pressure these same quantities are increased by a factor of roughly 1,000. A wide variation in $1/\mu$ exists for ultraviolet light, depending on wave length and nature of absorber. For the important case of chlorine, for a 1% unit density solution, $1/\mu$ is 0.1 cm. at 3,660Å. At the same wave length it is 1 cm. for gaseous chlorine at 0.36 atm. It appears that for all of these radiations except Co-60 gamma rays and beta particles, both in air at atmospheric pressure, optical thicknesses corresponding to a maximum mixing effect of 1% are readily attainable in photoreactors of reasonable size. A 10% effect is attainable for the same radiations in the annulus and the slab. Increases of 100% or more are possible with ultraviolet light, with beta particles in liquids, and with alpha particles and fission fragments. Measurable mixing effects may be found even with gamma rays and beta particles in gases at sufficiently high pressure.

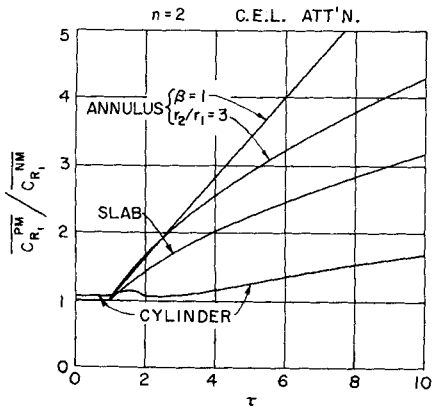

Fig. 6. Maximum effect of mixing, constant energy loss attenuation.

Table 5. Optical Thicknesses Corresponding to Various Levels of Maximum Mixing Effect

Main body of table contains values of τ corresponding to the maximum mixing effect possible stated as percentage increase in effluent product concentration or overall quantum yield based on incident intensity or on absorbed intensity.

Maximum mixing effect, %	Attenuation mode	Geometry			
		Cylinder	Slab	Annulus $\beta = 1$	Annulus $r_2/r_1 = 3$
1	Exp.	All	1	0.2	0.2
	C.E.L.	All	1	1	1
10	Exp.	12	3.4	2	2
	C.E.L.	3.4	1.2	1.1	1.1
100	Exp.	—	16	8	10.7
	C.E.L.	15	4	2.6	2.7

Dimensionless effluent product concentrations and overall quantum yields for second-order termination may be calculated using the expressions in Table 4 and Equations (13) to (16). The results of such calculations are shown graphically for exponential attenuation in Figures 7 to 10. In each of these figures two curves are shown for each geometry, one for each extreme state of mixing. For each such pair of curves, the ratio of the perfect mixing quan-

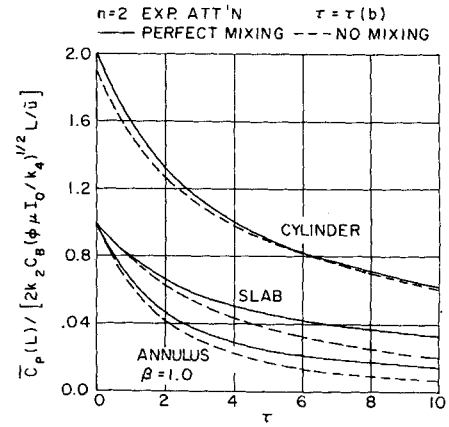

Fig. 7. Dimensionless mixed average effluent product concentration. Variation with b at constant μ [$\tau = \tau(b)$]. $n = 2$, exponential attenuation.

tity to that in the absence of mixing as a function of τ is identical with the corresponding relation given in Figure 5; and the discussion of this figure on relative magnitude of mixing effects applies to Figures 7 to 10 as well. Graphical representation of the results of the same calculations for constant energy loss radiation are available elsewhere (Figures 11 to 15 and the Appendix).*

Figures 7 and 8 show the dependence of dimensionless product concentration and quantum yield on reactor thickness. Figure 7 shows the product concentration. The variation with thickness is similar to that found for $n = 1$ and the order of the effect of geometry is also the same as for $n = 1$. Figure 8 shows the dimensionless quantum yield as a function of reactor thickness. The no mixing yields approach limits as the thickness increases, whereas the perfect mixing yields increase without limit. In the absence of mixing the intermediates are confined to the location at which they were produced. Therefore, increase in reactor thickness does not affect the concentration profile or rates of production at smaller thicknesses. Increase in thickness may produce additional absorption, or, in the case of the cylindrical reactor, it may introduce additional source surface. At sufficiently large thicknesses a negligibly small amount of additional production results from additional increases in thickness and the rate of production of product per unit of incident intensity, or Φ_o^{NM} approaches a limiting value. The limiting values for the slab and the cylinder are identical. The order of effect of geometry seen in Figure 7 is reversed in Figure 8. High product concentration is thus associated with low efficiency of source utilization and vice versa for $n = 2$.

The variation of dimensionless product concentration and quantum yield with absorption coefficient is shown in Figures 9 and 10. The same order of effect of geometry is present as was found previously. The perfect mixing curves approach limits as the absorption coefficient becomes large. The no mixing curves all exhibit maxima whose occurrence may be explained as follows. As in the case of first-order termination, at zero absorption coefficient there is no absorption and no conversion. As μ increases from zero, absorption occurs, and product is produced. In the absence of mixing, the chain carriers produced become confined to a smaller and smaller volume adjacent to the source as μ is increased, and the rate of the radical-radical termination reaction increases correspondingly. Eventually the enhanced rate of termination becomes more important than any further absorption, and a maximum in conversion and yield is established. With perfect mixing, the chain carriers are not confined to the location of their birth, but become uniformly distributed at a concentration corresponding to the mean initiation rate. When absorption is complete, the mean initiation rate reaches a maximum and limiting values of the conversion and quantum yield are attained.

The no mixing maxima are found at relatively small μ, and the values of the maximum product concentrations and quantum yields are major fractions of the perfect mixing limits. These observations suggest that for a given reactor, a given radiation source, and a given chemical system, it is possible to obtain optimum or nearly optimum conversion and quantum yield at small absorption coefficients regardless of the state of mixing. The same performance can be obtained at large μ but only in the presence of adequate mixing.

CHEMICAL AND MIXING TIME SCALES

The magnitudes of the mixing effect in the presence of radical-radical termination as just described are the maximum values obtainable, assuming that the two extremes of mixing are actually attainable. Some of the factors affecting this assumption will be discussed briefly in this section.

One mixing extreme corresponds to the absence of mixing and to the absence of appreciable diffusion. This extreme is probably most closely represented by the static batch reactor or by the laminar flow regime. Even in these circumstances, molecular diffusion is present, and, in addition, natural convection arising from concentration gradients (*18*), particularly in optically dense systems, may be present. Thus these cases represent only approximations to the no mixing extreme, although in certain instances they may be very good ones.

The condition of perfect mixing is reached when the mean chemical lifetime is long compared to times characteristic of mixing. The local mean lifetime of a chain for the mechanism under consideration in the absence of mixing is (*19*)

$$\theta_c^{NM}(\nu) = \frac{1}{2k_t C_{R_1}^{NM}(\nu)} = 1/\{2[k_s \phi I_a(\nu)]^{1/2}\}$$

In the case of the slab and the annulus, the minimum lifetime will be found adjacent to the source in the absence of mixing:

* See footnote on page 878.

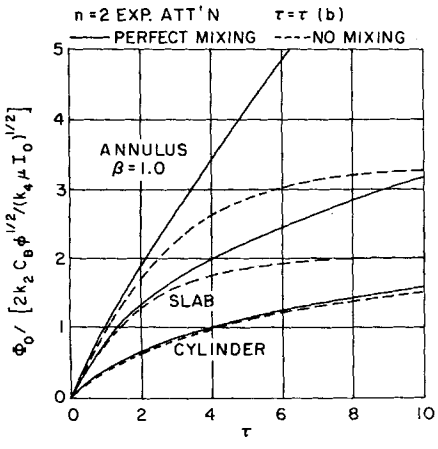

Fig. 8. Dimensionless overall quantum yield based on incident intensity. Variation with b at constant μ [$\tau = \tau(b)$]. $n = 2$, exponential attenuation.

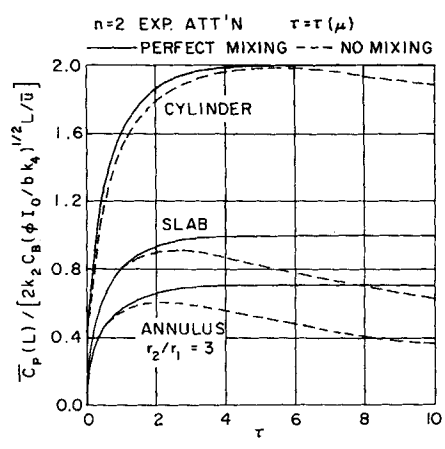

Fig. 9. Dimensionless mixed average effluent product concentration. Variation with μ at constant b [$\tau = \tau(\mu)$]. $n = 2$, exponential attenuation.

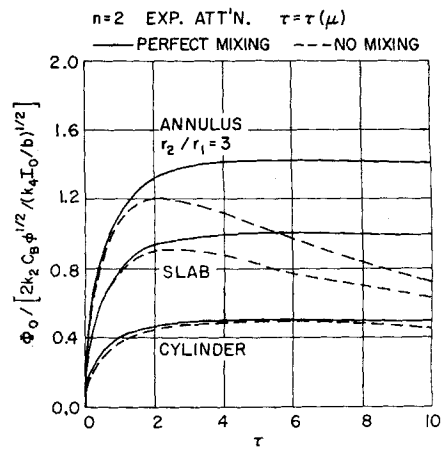

Fig. 10. Dimensionless overall quantum yield based on incident intensity. Variation with μ at constant b [$\tau = \tau(\mu)$]. $n = 2$, exponential attenuation.

$$\theta_C^{NM}(\sigma) = \frac{1}{2k_t C_{R_1}^{NM}(\sigma)} = 1/\{2[k_t p(0)\phi\mu I_o]^{1/2}\} \quad (17)$$

If the minimum lifetime is sufficiently long then, of course, all lifetimes will be long enough to permit realization of the perfect mixing extreme. For the cylinder, Equation (17) expresses either the maximum or an intermediate value of the chain lifetime, depending on attenuation mode and range of τ. With this fact in mind, Equation (17) may still serve to predict a measure of the chemical time scale in the cylinder as well as in the other two geometries.

One sees from Equation (17) the dependence of lifetime on absorption coefficient, on incident intensity, and on other quantities as well. Long lifetimes are favored by low intensities and by small absorption coefficients. With regard to the latter quantity, if one has a source of fixed dimensions and intensity in combination with a reactor of a given size, and if one can vary the absorption coefficient and the state of mixing at will, then with reference, say, to Figures 9 and 10, at sufficiently small μ, where the chemical lifetime is long, the perfect mixing condition can be attained. There is little if any difference between no mixing and perfect mixing at small μ (none for certain circumstances already pointed out), but nevertheless the state of perfect mixing can be realized there. In the continued presence of mixing as the absorption coefficient is increased, the perfect mixing curves may continue to be followed. They may be followed into the region in which there is a finite difference between the two mixing extremes, and they will be followed until the chemical lifetime begins to become comparable to or shorter than the mixing time. As the latter condition is approached, the effluent product concentrations and the quantum yields fall with increasing μ until the no mixing curves are reached, and they are subsequently followed. For high incident intensities the chemical lifetime may be too short to permit observance of a mixing effect at any value of μ, and the no mixing curves will be adhered to at all μ regardless of the degree of mixing. In any case a maximum effluent product concentration and a maximum quantum yield will be found as μ is increased from a very small value. A low intensity source will favor the perfect mixing curves and a high intensity source, the no mixing curves.

A rough idea of the practical attainability of the two mixing extremes may be found in estimates of characteristic chemical and mixing times. These are given in Table 6. In the first part of the table minimum lifetimes for chains with radical-radical termination calculated from Equation (17) are given. The range of termination rate constants examined runs from the high value of 10^{11} liter/mole-sec. found for the preexponential factor in gas phase bimolecular reactions of simple molecules down to the value of 10^{7} liter/mole-sec., of the order of magnitude reported for some chlorinated hydrocarbon radical-radical reactions in solution and for some bulk polymerization reactions (*20*).

A measure of the time scale of mixing is given by

$$\theta_M = b^2/2D \quad (18)$$

It is assumed in Equation (18) that whether on a molecular or macroscopic scale, the mixing process may be characterized as a diffusion process. Values of θ_M are given in the second part of Table 6.

The lower value used for the apparent diffusion coefficient is included in the range of molecular diffusion coefficients in liquids, while the upper one is in the range of the same coefficients for gases. Turbulent radial eddy diffusion coefficients of the order of 1 sq. cm./sec. have been reported for mixing in liquids in tubular conduits (*21*). We see in Table 6 that the large mixing times associated with apparent diffusion coefficients of the order of 10^{-5} sq. cm./sec., relative to all of the chemical times shown, would normally assure that static liquids or the regime of laminar flow in liquids would probably always correspond to the case of no mixing. The superposition of natural convection would, however, produce a substantial decrease in θ_M so that a general statement cannot be made. The values of θ_M corresponding to the higher value of D relative to the values shown for $\theta_C^{NM}(\sigma)$ indicate that the perfect mixing condition might be attained in relatively thin reactors involving gases in laminar or turbulent flow and liquids in turbulent flow.

TABLE 6. CHAIN LIFETIMES AND MIXING TIMES

(*a*) Lifetimes for chains with radical-radical termination calculated from Equation (17) with $p(0) = 1$

$C_{R_1}^{NM}(\sigma)$, mole/liter	k_t, liter/mole-sec. 10^{7}	10^{9}	10^{11}
	$\theta_C^{NM}(\sigma)$, sec.		
10^{-9}	0.5×10^{2}	0.5	0.5×10^{-2}
10^{-7}	0.5	0.5×10^{-2}	0.5×10^{-4}
10^{-5}	0.5×10^{-2}	0.5×10^{-4}	0.6×10^{-6}

(*b*) Characteristic mixing times calculated from Equation (18)

D, sq. cm./sec.	b, cm. 1	10	100
	θ_M, sec.		
10^{-5}	0.5×10^{5}	0.5×10^{7}	0.5×10^{9}
10^{0}	0.5	0.5×10^{2}	0.5×10^{4}

SUMMARY

1. The system of material balances for a photoinitiated chain reaction was formulated and solved, taking into account the presence of radiation attenuation, type of chain termination step, photoreactor geometry, and state of mixing. Stationary state kinetics and low conversion were assumed.

2. It was formally shown that for a chain termination step, which is first order with respect to chain carrier, there is no effect of mixing. For second-order termination, it was shown that in the presence of radiation attenuation, and with chain lifetimes that are long compared to mixing times, the introduction of mixing results in increased conversion and overall quantum yield. Further, if mixing is introduced step-by-step, first in one direction of radiation attenuation and then in a second such direction as well, increased performance follows each step.

3. The variation of conversion and overall quantum yield with reactor thickness and with absorption coefficient was calculated for photoreactors having monoenergetic, unidirectional sources, and for first- and second-order termination. For second-order termination at large optical thicknesses, the maximum relative effect of mixing increased with optical thickness, and it increased with attenuation mode in the order exponential attenuation, constant energy loss attenuation, and with reactor geometry in the order cylinder, slab, and annulus.

4. Combinations of type of radiation and reactant phase were pointed out in which measurable mixing effects might be found, based on magnitude of optical thickness. The circumstances under which chemical lifetimes may be found to be long compared to mixing times were discussed. It was pointed out that regardless of mixing state for a given combination of reactor, source, and chemical system, maximum values of the effluent product concen-

tration and overall quantum yield will be found as a result of varying the absorption coefficient.

5. The circumstances under which mixing effects are predicted appear to be consistent with industrial experience (*1* to 5), though the origin of industrially encountered mixing effects has by no means been conclusively identified. The present analysis may nevertheless serve as a basis for the systematic study of mixing effects.

ACKNOWLEDGMENT

This work was performed under the auspices of the U. S. Atomic Energy Commission.

The authors express appreciation to Leonard Geller, who suggested the use of the Schwarz inequality; to T. J. Krieger for discussion and clarification of mathematical matters; and to D. T. Lee and J. A. Mahoney for useful comments.

NOTATION

b = reactor thickness, cm. (see Table 1)
C_i = concentration of i, moles/liter
$\overline{C}_i$ = average concentration of i, moles/liter
D = effective diffusion coefficient, sq. cm./sec.
F = volumetric flow rate, liter/sec.
I_a = rate of absorption of radiation, einstein/liter-sec.
$\overline{I}_a$ = average rate of absorption of radiation, einstein/liter-sec.
I_o = rate of incidence of radiation on reactant at location σ, einstein/(liter/cm.)-sec.
k_i = initiation rate constant, sec.$^{-1}$
k_p = propagation rate constant, liter/mole-sec.
k_t = generalized rate constant for termination reaction, (mole/liter)$^{1-n}$/sec.
k_2,k_3,k_4,k_5 = rate constants of propagation and termination reactions, liter/mole-sec.
L = length of radiation source in flow direction, that is, length of photoreactor, cm.
n = order of termination reaction, dimensionless
$p(\tau)$ = dimensionless function defined in Tables 2 and 3
$P(\nu)d\nu$ = differential element of flow cross section: wdx for the slab, and $2\pi rdr$ for the annulus and the cylinder, sq. cm.
$q(\tau)$ = dimensionless function defined in Tables 2 and 3
r = radial distance, cm.
r_o = radius of cylinder, cm.
r_1,r_2 = inner and outer radii of annulus, respectively, cm.
R = range of heavy particle, cm.
$\overline{R}$ = dimensionless average radius (see Table 1)
S = flow cross section, sq. cm.
t = time, sec.
$u(\nu)$ = velocity at location ν in z direction, cm./sec.
$\overline{u}$ = velocity averaged over flow cross section, cm./sec.
V = reactor volume, liter
w = width of slab source, cm.
x = distance coordinate normal to slab source, cm.
x_1 = thickness of slab reactor, cm.
z = distance coordinate in direction parallel to source surface, cm.

Greek Letters

α = molar absorption coefficient, base e, liter/mole-cm.
β = μr_1, dimensionless radius of source in annular reactor
θ_C = mean chemical lifetime, sec.
θ_M = characteristic mixing time, sec.
μ = linear absorption coefficient, cm.$^{-1}$
ν = generalized distance coordinate normal to source surface, cm.
ν_1,ν_2 = limits of variation of ν coordinate, cm.
ρ = generalized dimensionless distance coordinate normal to source
σ = generalized location of source along ν coordinate, cm.
τ = μb, optical thickness, dimensionless
ϕ = primary quantum yield, moles of A dissociated per einstein absorbed
Φ_o,Φ_a = overall quantum yield of P based on incident and absorbed intensity, respectively, mole/einstein

Superscripts

NM = absence of mixing in all directions
PM = state of perfect mixing in ν direction with absence of mixing in z direction
$*$ = state of perfect mixing throughout reactor

LITERATURE CITED

1. Anderson, Jr., William T., *Ind. Eng. Chem.*, **39**, 844-846 (1947).
2. N. V. de Bataafsche Petroleum Maatschappij, Brit. Pat 660072 (October 31, 1951).
3. Governale, L. J., and J. T. Clarke, *Chem. Eng. Progr.*, **52**, 281-285 (1956).
4. Anonymous, *Ind. Eng. Chem.*, **54**, No. 8, 20-28 (1962).
5. Rosenberg, David S., "Chlorine, Its Manufacture, Properties and Uses," J. S. Sconce, ed., pp. 625 to 629, Reinhold, New York (1962).
6. Bhagwat, W. V., and N. R. Dhar, *J. Indian Chem. Soc.*, **9**, 335-340 (1932).
7. Noyes, William A., and Philip A. Leighton, "The Photochemistry of Gases," pp. 187-198, Reinhold, New York (1941).
8. *Ibid.*, pp. 200-202.
9. Syrkus, N. P., *Dokl. Akad. Nauk* SSSR, **152**, 1185-1188 (1963).
10. Davis, E. A., "Algal Culture from Laboratory to Pilot Plant," John S. Burlew, ed., p. 135, Carnegie Institute of Washington Publ. No. 600, Washington, D. C. (1953).
11. Frederickson, A. G., A. H. Brown, R. L. Miller, and H. M. Tsuchiya, *Am. Rocket Soc. J.*, **31**, 1429-1435 (1961).
12. Huff, James E., and Charles A. Walker, *A.I.Ch.E. J.*, **8**, 193-200 (1962).
13. Shuler, R. H., *J. Phys. Chem.*, **62**, 37-41 (1958).
14. Kaplan, W., "Advanced Calculus," Addison-Wesley, Reading, Massachusetts (1952).
15. Hill, T. L., *J. Chem. Phys.*, **17**, 1125-1131 (1949).
16. Pritchard, H. O., and G. O. Pritchard, *Can. J. Chem.*, **41**, 3042-3049 (1963).
17. Schlechter, R. S., and E. H. Wissler, *Appl. Sci. Res.*, **A9**, 334-344 (1960).
18. Baginski, F. C., D. Eng. dissertation, Yale Univ., New Haven, Connecticut (1952).
19. Burnett, G. M., and H. W. Melville, "Technique of Organic Chemistry," Arnold Weissberger, ed., Vol. VIII, 2 ed., Part II, pp. 1100-1111, Interscience, New York (1963).
20. Benson, S. W., "The Foundations of Chemical Kinetics," Tables XV.1 and XVI.3, McGraw-Hill, New York (1960).
21. Seagrave, Richard C., and R. W. Fahien, "Turbulent Mass Transfer in Liquid Streams," U. S. Atomic Energy Commission Rept. IS-419, Ames Laboratory, Iowa State Univ., Ames, Iowa (1961).
22. Von Halban, H., and K. Siedentopf, *Z. Phys. Chem.*, **103**, 71-90 (1922).
23. Glasstone, S., "Principles of Nuclear Reactor Engineering," Van Nostrand, Princeton, New Jersey (1955).
24. Price, William J., "Nuclear Radiation Detection," p. 18, McGraw-Hill, New York (1958).
25. Lind, S. C., "Radiation Chemistry of Gases," Reinhold, New York (1961).

Manuscript submitted February 16, 1965; revision received May 13, 1965; paper accepted May 17, 1965. Paper presented at A.I.Ch.E. Boston meeting.